Virtual Magnetic TL-based Channel Modeling of SWIPT Systems assisted by MTMs

Jorge Virgilio de Almeida, Eduardo Costa da Silva and Marbey Manhães Mosso
Dept. of Electrical Engineering
Pontifical Catholic University of Rio de Janeiro
Rio de Janeiro, Brazil
virgilio@aluno.puc-rio.br

Carlos A. F. Sartori
Dept. of Electrical and Automation Engineering
Polytechnic School of University of São Paulo
São Paulo, Brazil
Nuclear and Energy Research Institute
University of São Paulo
São Paulo, Brazil

***Abstract*— This paper describes a general methodology for the description of inductive power and data transfer based on virtual magnetic transmission-lines (VMGTLs). This approach presents a better physical insight on the channel behavior since the model correctly preserves the energy flow between the transmitting and receiving coils. Particularly, the virtual-TL analogy clarifies the mechanism of transmission gain improvement between any two coils assisted by MTM lenses. Based on the results of this work, these lenses do not enhance the magnetic coupling between the drivers, as usually claimed, but create conditions to propagating near-field modes to increase their power transfer. This approach also reveals that MTMs could be employed not only for the increasing of power transfer but also for enlarging the inductive channel bandwidth.**

Keywords*— *SWIPT, IoT, inductive channel, metamaterial, virtual magnetic transmission lines

I. INTRODUCTION

Inductive-coupling based systems present enormous advantages over other power and data transmission mechanisms like electromagnetic (EM) or acoustic propagating waves in extreme environments, such as underground or underwater, due to the fact that the vast majority of the materials in the Universe are magnetic insensitive (this is to say, their permeability equals the free-space one). For this reason, the envisioned Internet of Underwater and Underground Things (IoUT) are expected to primarily rely on inductive channels [1-3]. Despite of their virtues, however, their fundamental flaws remain a challenge for designers. Particularly, their very limited operation range and strictly nonlinear nature. In the last decades, many different techniques have been proposed trying to ameliorate or mitigate such problems. Concerning the limitations in the operating range, the main strategies employed by designers are: resonant relays [4-6] or near-field MTM based lenses [7-9].

Both strategies are actually quite similar to each other since both employ very frequency-selective circuits (high-Q resonators) in order to compensate the magnetic-coupling decaying. According to [10], the MTM solution differs from the previous one due to its "lattice gain", which emerges from the collective behavior of its unit-cells. In both cases, however, the common-used analytical method consists on solving a set of linear equations relating the circuit component of the drivers (resistance, inductance, capacitance, etc), which can be highly complex to solve, particularly when MTM (artificial crystals made out of many small resonant coils) are involved. Also, there is a fundamental problem in taking this approach, since, as it be further shown here, coupling is not the unique power transfer mechanism of the near field. This oversimplification usually conducts to the wrong conclusion that assumes signal variance and power to be exactly the same thing in simultaneous wireless power and data transmission (SWIPT). It is a core problem for these systems since their control and tuning depends on the knowledge of the channel.

Some papers have tried to overcome this problem by directly characterizing the inductive channel through measurement [11]. Yet this strategy is also quite complicated to be implemented, especially considering operating scenarios like massive MIMO-SWIPT. Based on that, a more systematic inductive channel modeling technique based on virtual magnetic transmission line (VMGTL) is proposed in order to solve large-scale systems. This model was recently introduced in [12] as an extension of the theory of the magnetic TLs for non-confined magnetic flux. Like the Gyrator-Capacitor Lumped Element Model [13], VMGTL also preserves the representation of the energy flow along the inductive channel, with the advantage of being a distributed model.

In this paper, VMGTL-based channel modeling is employed to make a parametric study of the impact of the insertion of MTM lenses in the magnetic link. The obtained results show that MTM-assisted inductive channels can also transfer power by means of backward propagating modes and that in fact it is these modes that are responsible for MTM-enhanced coupling phenomenon.

II. Channel Modeling using a Virtual Magnetic Transmission Line Approach

In this section, VMGTL technique is briefly presented and some parametric studies are done in order to clarify the inductive channel response to MTM-based artificial magnetic conductors. This theoretical development is the same one previously introduced by the authors in [12].

A. Inductive Channel Modeling using VMGLT

The main design principal of the VMGTL model is the observation that electric/magnetic fluxes and charges have the same dimension. Hence, any time-varying flux behaves as a "virtual current" (which are the well-known displacement magnetic/electric currents):

$$j\omega\phi_m = j\omega \iint \boldsymbol{B}\cdot d\boldsymbol{s} = \iint j\omega\boldsymbol{B}\cdot d\boldsymbol{s} = \iint \boldsymbol{J}_{m,d}\cdot d\boldsymbol{s} = I_{m,d} \quad [V] \tag{1}$$

$$j\omega\phi_e = j\omega \iint \boldsymbol{D}\cdot d\boldsymbol{s} = \iint j\omega\boldsymbol{D}\cdot d\boldsymbol{s} = \iint \boldsymbol{J}_{e,d}\cdot d\boldsymbol{s} = I_{e,d} \quad [A] \tag{2}$$

Like real current, displacement ones can also guide EM fields, as illustrated in Fig. 1.

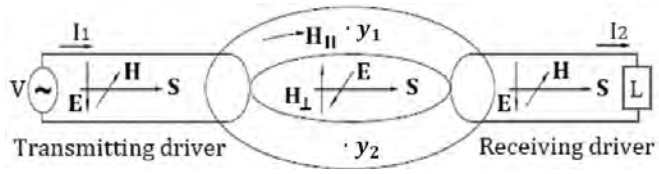

Fig. 1. The displacement magnetic current $I_{m,d}$ between the transmitting and receiving coils forms a virtual circuit similar to a conventional TL. Accordingly to Poynting theorem, power flow in the inductive channel will depends on the perpendicular component of the magnetic near field created by the magnetic potential difference between the flux in positions y_1 and y_2.

For all purpose, a VMGTL consists of two insulated drivers with no physical charge flowing between them and interacting only by means of non-confined magnetic flux. The driving force of a VMGTL is the magnetic potential V_m given by:

$$V_m = \int_{y_1}^{y_2} \boldsymbol{H}_\perp(\omega)\cdot d\boldsymbol{l} \tag{3}$$

The magnetic potential V_m and the magnetic displacement current $I_{m,d}$ of the VMGTL follow propagation equations analogous to the ones of conventional TLs:

$$\frac{d}{dz}V_m(z) = \left(\frac{\mathcal{R}'_m}{j\omega} + G'_e\kappa_m^2 + j\omega C'\kappa_m^2\right) I_{m,d} = Z_m I_{m,d}(z) \quad \left[\frac{A}{m}\right] \tag{4}$$

$$\frac{d}{dz}I_{m,d}(z) = (G'_m\kappa_m^2 + j\omega L'\kappa_m^2)V_m = Y_m V_m(z) \quad \left[\frac{V}{m}\right] \tag{5}$$

where Z_m, Y_m, $\mathcal{R}'_m$, κ_m, G'_e, G'_m, L' and C' denote the series magnetic impedance, the shunt magnetic admittance, the magnetic reluctance, the magnetic coupling coefficient, the electrical conductance, the magnetic conductance, the inductance and the capacitance per unit length, respectively.

From Eqs. 4-5, it can be seen that when $\kappa_m \to 1$ the TL analogy becomes quite similar to the magnetic TLs proposed by [14]. VMGTL approach, however, keeps its validity even when κ_m is low until the limiting case where $Y_m \to 0$.

The characteristic electrical impedance Z_0 of the VMGTL, its complex propagation parameter γ and its load reflection coefficient Γ are defined as:

$$Z_0 = \frac{I_{m,d}(z)}{V_m(z)} = \sqrt{\frac{Y_m}{Z_m}} = \sqrt{\frac{G'_m + j\omega L'}{\frac{\mathcal{R}'_m}{j\omega} + G'_e + j\omega C'}} \quad [\Omega] \tag{6}$$

$$\gamma = \sqrt{Z_m Y_m} = \sqrt{\left(\frac{G'_m}{j\omega} + L'\right)\left(-\frac{\mathcal{R}'_m}{\omega^2} + \frac{G'_e}{j\omega} + C'\right)} \quad \left[\frac{rad}{m}\right] \tag{7}$$

$$\Gamma = \frac{Z_{RX} - Z_0}{Z_{RX} + Z_0} \tag{8}$$

where Z_{RX} is the load at the receiver. The general solution of this one-dimensional Helmholtz problem is [15]:

$$I_m(z) = I_m(0)e^{-\gamma z}(1 + \Gamma e^{2\gamma z}) \quad [V], \tag{9}$$

$$V_m(z) = \frac{I_m(0)}{Z_0}e^{-\gamma z}(1 - \Gamma e^{2\gamma z}) \tag{10}$$

The total power flow at any point of the inductive channel will then be:

$$P_f(\omega) = V_m I^*_{m,d} \quad [W] \tag{11}$$

By definition, the frequency-domain channel transfer function of the system is given by:

$$H(\omega) = \frac{V_m(0)}{V_m(-l)} = \frac{e^{-\gamma D}(1 - \Gamma)}{(1 - \Gamma e^{-2\gamma D})} \tag{12}$$

where D is the separation distance of the drivers.

It is important to mention that the model is only valid if $D > r^{TX}/2$, where r^{TX} is the radius of TX coil.

B. Estimation of the Model Parameters

In order to determine the five parameters presented in Eqs. 4-5, some simplifying hypotheses must be made.

The first hypothesis assumes that distributed elements G'_e, G'_m, L' and $C'$are uniform throughout the inductive channel. If so, they can be directly estimated as follows:

$$L' = \frac{L_0}{D} \tag{13}$$

$$C' = \frac{C_0}{D} \tag{14}$$

$$G'_e = \omega C' \frac{Im\{\varepsilon_r\}}{Re\{\varepsilon_r\}} \tag{15}$$

$$G'_m = \omega L' \frac{Im\{\mu_r\}}{Re\{\mu_r\}} \tag{16}$$

where L_0 and C_0 are the equivalent inductance and capacitance of the TX coil, and ε_r and μ_r are the relative permittivity and permeability of the channel medium.

The estimation of distributed $\mathcal{R}'_m$, however, is a little bit more complicated, since the original concept of magnetic reluctance $\mathcal{R}_m$ was conceived for magnetic circuits where most of the magnetic flux is confined into a region of constant transverse section imposed by a ferromagnetic core. Nevertheless, despite of that, an approximation for the non-confined case can be made.

First, we observe that, by definition, $\mathcal{R}_m$ is given by:

$$\mathcal{R}_m = \frac{V_m}{\phi_m} \tag{17}$$

where V_m and ϕ_m is the TX-coil magnetic-motive force of the transmitter and the mutual flux between the TX and the RX.

Secondly, we recall that the mutual inductance M_{RX-TX} between the drivers is given by:

$$M_{RX-TX} = \frac{\phi_m^{RX-TX}}{V_m^{TX}} \tag{18}$$

Hence, based on Eqs. 17-18, $\mathcal{R}'_m$ can be approximated by:

$$\mathcal{R}'_m \propto \frac{1}{M^{RX-TX}\xi} \tag{19}$$

where ξ is a geometrical weighting parameter.

Making another simplifying hypothesis that ξ equals the square of the radius of TX-coil

$$\xi \cong r^2 \tag{20}$$

the equivalent VMGTL of the system can now be completely characterized.

C. MTM interaction with the Inductive Channel

As demonstrated in [12], the effects of the MTM on the inductive channel can be introduced to the VMGTL model by defining an equivalent impedance of the MTM.

Assuming MTM slabs made of a constant lattice of spiral resonators (SRs) unit cells, the equivalent Z_{MTM} is found to be:

$$Z_{MTM}(\omega) = j\omega a\mu_0 \left(1 - \boldsymbol{sign}(\kappa_m)\frac{F\omega^2}{\omega^2 - j\omega\omega_0/Q - \omega_0^2}\right) \tag{21}$$

where a and ω_0 are the period of the MTM lattice and its operating angular frequency, and F and Q are the filling factor and the quality factor of the unit cells.

Hence, Eq. 5 can be rewritten as

$$\frac{d}{dz}I_{m,d}(z) = \left(G'_m\kappa_m^2 + j\omega L'\kappa_m^2 + Z_{MTM}(\omega)\kappa_{m,MTM}^2\right)V_m = Y_m V_m(z) \quad \left[\frac{V}{m}\right] \tag{22}$$

since the MTM changes the variation of the magnetic flux with the distance. In other words, the MTM alters the magnetic admittance Y_m of the channel.

The magnetic coupling between the MTM and the TX and RX coils depends on the physical size of the MTM. Assuming a semi-infinite MTM plane in the transversal section of the channel, it can be approximated by:

$$\kappa_{m,MTM} \cong 2\kappa_m \tag{23}$$

This simplifying hypothesis can be assumed if the MTM dimensions are larger than the diameter TX and RX coils.

III. Model Application and Discussion

The considered system is composed of two electrically small far-from-resonance coils separated by a fixed distance $D = 15cm$. The coils are copper-made with diameter $p = 1\,\text{mm}$. The self-inductance L_0 of the small circular loop is found in closed-form in literature [16]. Their magnetic coupling coefficient κ_m can be estimated using the thin-wire approximation [17]. In the present work, all the MTM slabs are made of square SRs identical to the one employed in [12], with the same equivalent Z_{MTM}. Also, they are supposed to be placed perpendicularly to the magnetic flux.

In order to demonstrate the model's accuracy, the analytical channel estimation is compared with the one obtained on ADS2019 using the Method of Moments. Notice that some discrepancies between the analytical and the numerical results exist due to the simplifying hypotheses applied to Eqs. 19-23.

As shown in Fig. 4, when there is no MTM in the channel, imaginary part of the propagation constant γ, known as phase constant β, is null, and the real part of γ, known as the attenuation constant α, is low-varying with frequency. In this situation, the only mechanism of power exchange between the electric interfaces is their mutual coupling. The H-field lines generated by each driver are in contact with its neighbor, hence inducing current on it accordingly to Faraday's Law. This case can be completely characterized by means of the mutual inductance matrix and similar circuital analogies.

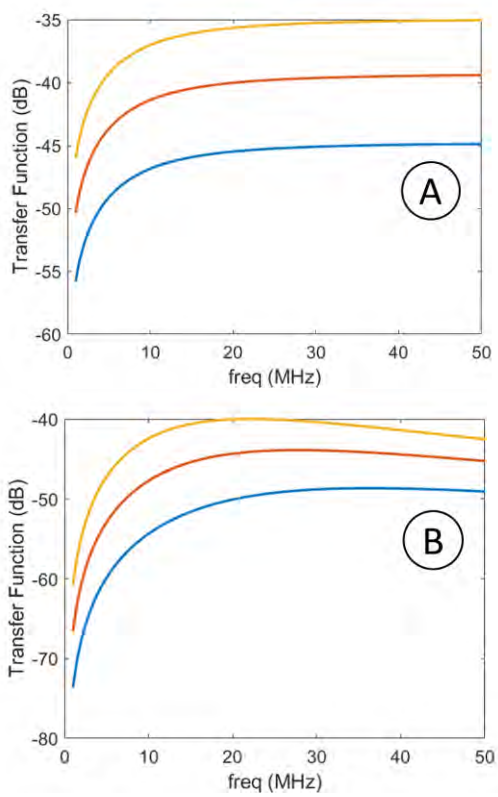

Fig. 2. Magnitude of the transfer function as a function of frequency for a VGMTL without MTM: analytical model (a) and numerical simulation (b) for r=4cm (blue), r=5cm (orange) and r=6cm (yellow).

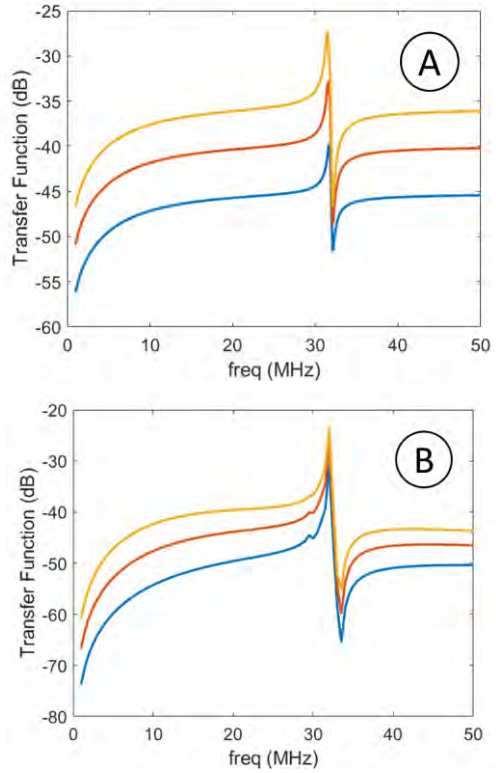

Fig. 3. Magnitude of the transfer function as a function of frequency for a VGMTL assisted by one MTM slab: analytical model (a) and numerical simulation (b) for $r = 4$cm (blue), $r = 5$cm (orange) and $r = 6$cm (yellow).

However, if a MTM slab is introduced in the channel, independently of its relative position inside the link, other power transfer mechanisms arises. In Fig. 5, it can be seen that the enhancement of the transmission gain around the MTM operating frequency f_0 is basically due to the appearance of a pass-band (non-null propagation constant) in the inductive link. So, the additional power being transferred between the drivers is not coming from the enhancement of the coupling, but by propagating modes supported by the MTM lens. Notice that since ($\beta < 0$) these waves are backwardly-oriented ones.

Another important fact usually neglected by the literature on MTM-enhanced coupling theory and that becomes clear with this approach is the region of minimum attenuation in the MTM-induced pass-band. This region lies in the sub-resonant region and has a relative flat response in comparison with the region of maximum power gain (around the operating frequency f_0). This means that this region imposes very low distortion to signals and can be used for improved data transmission.

Thus, we can conclude that MTMs could be either used for maximizing data rate or power transfer, but optimum values for both cannot be simultaneously obtained. Optimum bandwidth-gain trade-off in SWIPT systems lies in-between this two cases.

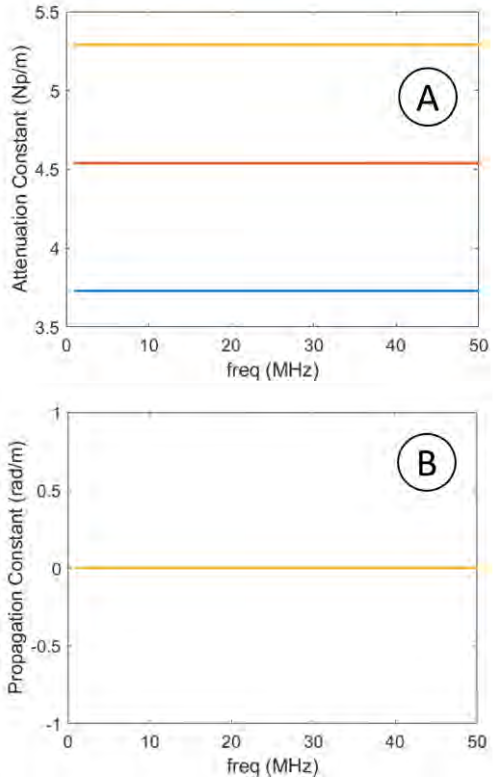

Fig. 4. Attenuation (a) and propagation (b) constants as a function of frequency for a VGMTL without MTM for $r = 4$cm (blue), $r = 5$cm (orange) and $r = 6$cm (yellow).

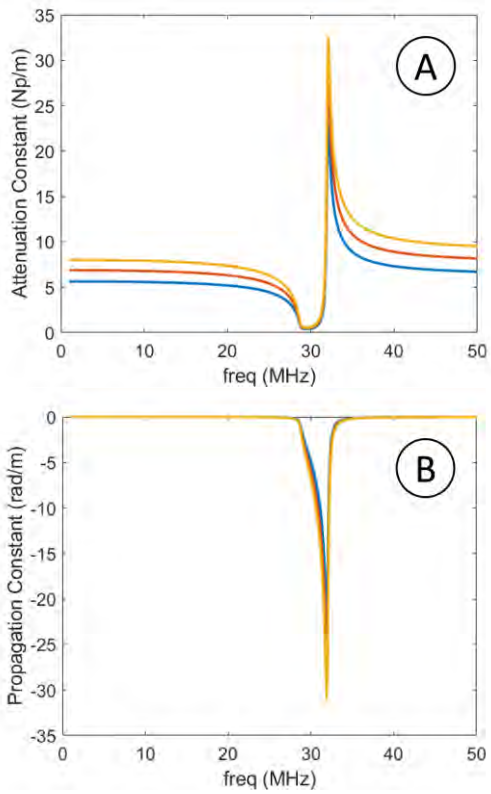

Fig. 5. Attenuation (a) and propagation (b) constants as a function of frequency for VGMTL assisted by one MTM slab for $r = 4\text{cm}$ (blue), $r = 5\text{cm}$ (orange) and $r = 6\text{cm}$ (yellow).

IV. Conclusion

In this work, a VGMTL-based model of the channel was employed in order to clarify the MTM mechanism of power enhancement. Metamaterial-enhanced coupling is shown to be actually a secondary power transfer supported by backward propagating modes around the resonance. Besides that, the VMGTL model has demonstrated the existence of a flat minimum-distortion response in the sub-resonance region of the system that could be employed to maximize the bandwidth/data rate. This region, however, is show to have just a slight power gain in comparison with the inductive channel assisted by no MTM. Although passive MTMs can only maximize either the power transfer or the data rate, it remains as a possibility that active MTMs, with electronically controlled unit-cells, could be employed in order to create reliable SWIPT networks in extreme environments, such as future the Internet of Underwater Things (IoUT), that could switch from one region to the other (high-gain or minimum distortion) accordingly to the system operation. Finally, in a future work, the authors intend to present a complete parametric study of inductively-coupled SWIPT systems, as well as an extension of this theory to MIMO scenarios.

Acknowledgements

The authors would like to thank CNPq for the financial support and the reviewers for their valuable comments.

References

[1] K. M. Awan, P. A. Shah, K. Iqbal, S. Gillani, W. Ahmad and Y. Nam, "Underwater Wireless Sensor Networks: A Review of Recent Issues and Challenges," *Wireless Communications and Mobile Computing,* vol. 2019, no. 6470359, p. 20, 2019.

[2] R. Guida, E. Demirors, N. Dave, J. Rodowicz and T. Melodia, "An Acoustically Powered Battery-less Internet of Underwater Things Platform," in *2018 Fourth Underwater Communications and Networking Conference (UComms)*, Lerici, Italy, 2018.

[3] N. Khalil, M. R. Abid, D. Benhaddou and M. Gerndt, "Wireless sensors networks for Internet of Things," in *2014 IEEE Ninth International Conference on Intelligent Sensors, Sensor Networks and Information Processing (ISSNIP)*, Singapore, Singapore, 2014.

[4] D. C. Corrêa, U. C. Resende and F. S. Bicalho, "Experiments With a Compact Wireless Power Transfer System Using Strongly Coupled Magnetic Resonance and Metamaterials," *IEEE Transactions on Magnetics,* vol. 55, no. 8, 2019.

[5] D. Ahn, M. Kiani and M. Ghovanloo, "Enhanced Wireless Power Transmission Using Strong Paramagnetic Response," *IEEE Transactions on Magnetics,* vol. 50, no. 3, 2014.

[6] F. Zhang and M. Sun, "Efficient Wireless Power Transfer based on Strongly Coupled Magnetic Resonance," in *Wireless Power Transfer*, 2 ed., River Publishers, 2016, pp. 73 - 104.

[7] B. Wang, W. Yerazunis and K. Teo, "Wireless Power Transfer: Metamaterials and Array of Coupled Resonators," *Proceedings of the IEEE,* 2013.

[8] Y. Urzhumov and D. R. Smith, "Metamaterial-enhanced coupling between magnetic dipoles for efficient wireless power transfer," *Phys. Rev. B,* vol. 83, no. 205114, pp. 1 - 10, 2011.

[9] P. Sharma, D. Bhatia and R. S. Meena, "Metamaterial enhanced magnetization induced communication for wireless applications," in *2017 International Conference on Information, Communication, Instrumentation and Control (ICICIC)*, Indore, India , 2017.

[10] J. V. de Almeida and R. S. Feitoza, "Metamaterial-Enhanced Magnetic Coupling: An Inductive Wireless Power Transmission System Assisted by Metamaterial-Based Mu-Negative Lenses," *IEEE Microwave Magazine,* vol. 19, no. 4, pp. 95 - 100, 2018.

[11] T. Arakawa, S. Goguri, J. V. Krogmeier, A. Kruger, D. J. Love, R. Mudumbai and M. A. Swabey, "Optimizing Wireless Power Transfer FromMultiple Transmit Coils," *IEEE Access,* vol. 6, pp. 23828 - 23838, 2018.

[12] J. V. de Almeida, G. L. Siqueira, M. M. Mosso and C. A. F. Sartori, "Mu Negative Metamaterials Seen as Band Limited Non Foster Impedances in Inductive Power Transmission Systems," *Journal of Microwaves, Optoelectronics and Electromagnetic Applications,* vol. 18, no. 4, pp. 492 - 504, 2019.

[13] D. C. Hamill, "Lumped Equivalent Circuits of Magnetic Components: The Gyrator-Capacitor Approach," *IEEE Transactions on Power Electronics,* vol. 8, no. 2, pp. 97 - , 1993.

[14] J. A. B. Faria and M. P. Pires, "Theory of Magnetic Transmission Lines," *IEEE Transactions on Microwave Theory and Techniques,* vol. 60, no. 10, pp. 2941-2949, 2012.

[15] R. F. Harrington, Time-Harmonic Electromagnetic Fields, Piscataway, NJ: Wiley-IEEE Press, 2001, pp. 61-66.

[16] C. A. Balanis, Antenna Design Theory, Hoboken, New Jersey: John Wiley & Sons, Inc, 2005.

[17] R. M. Duarte and G. K. Felic, "Analysis of the Coupling Coefficient in Inductive Energy Transfer Systems," *Active and Passive Electronic Components,* vol. 2014, Article ID 951624, 6 pages, 2014.